Discovery of a potent cytotoxic agent that promotes G_2/M phase cell cycle arrest and apoptosis in a malignant human pharyngeal squamous carcinoma cell line

MANUNYA NUTH[1], MANJUNATHA R. BENAKANAKERE[1] and ROBERT P. RICCIARDI[1,2]

[1]Department of Basic and Translational Sciences, School of Dental Medicine; [2]Abramson Cancer Center, Perelman School of Medicine, University of Pennsylvania, Philadelphia, PA 19104, USA

Received September 1, 2021; Accepted January 31, 2022

DOI: 10.3892/ijo.2022.5331

Abstract. Squamous cell carcinoma is the major form of malignancy that arises in head and neck cancer. The modest improvement in the 5-year survival rate underpins its complex etiology and provides the impetus for the discovery of new therapeutics. The present study describes the discovery of an indole-based small molecule (24a) that was a potent cytotoxic agent with antiproliferative and pro-apoptotic properties against a pharyngeal carcinoma cell line, Detroit 562, effectively killing the cells at a half-maximal inhibitory concentration of 0.03 μM, as demonstrated using cell proliferation studies. The antiproliferative property of 24a was demonstrated by its ability to promote G_2/M blockade, as assessed by cell cycle analysis using flow cytometry and the monitoring of real-time cell cycle progression by the fluorescence ubiquitination-based cell cycle indicator. This pro-apoptotic property is supported by the promotion of TUNEL-staining and increase in the activities of caspases-3/7 and -6, in addition to the expression of death receptors and the cleavage of poly (ADP-ribose) polymerase 1 protein as demonstrated by western blotting. Given that Detroit 562 lacks functional p53, it is suggested that 24a acts independently of the tumor suppressor.

Introduction

It is estimated that >90% of cancers of the head and neck regions are squamous cell carcinomas (HNSCC) that arise from the oral cavity, pharynx and larynx (1). Alcohol and tobacco use (2) and human papillomavirus exposure (3) are important risk factors. As of 2018, cancer of the pharynx accounts for 1.7% of all cancer-related mortalities worldwide (4). While the underlying mechanisms for the development of HNSCC are complex (5), the tumor suppressor p53 plays an important role in antagonizing the initiation and progression of numerous cancers. By contrast, its alterations can lead to the impairment of the cell cycle checkpoint and represent the early events in progression observed for HNSCC cancers (6). Mutations at the DNA-binding domain are considered particularly disruptive and are associated with poor prognosis (7). Indeed, TP53 is the most frequently mutated gene observed in HNSCC-derived cells (69.9%) (8).

Standard treatment modalities for HNSCC tumors consist of surgery, radiotherapy and chemotherapy that are often accompanied by considerable morbidity (9). Despite the improvement in curative efforts, the 5-year survival rate remains relatively constant at ~66% for all cancer stages (10). While surgery is the primary option, numerous patients present with advanced diseases that preclude resection and are only accessible to radiotherapy and chemotherapy. As such, an important and commonly used chemotherapy is the cytotoxic platinum-based drug, cisplatin (11). Cisplatin has been used to treat various cancers, such as biliary tract and breast cancer, carcinoma of salivary gland origin, cervical, colon, gastric and lung cancer, melanoma, prostate and pancreatic cancer, squamous cell carcinoma of male genital tract and urothelial bladder cancer (12). In regard to unresectable oral squamous cell carcinoma tumors, cisplatin is recommended as a standard agent in combination with radiation (13). However, drug-resistance and significant toxicity pose concerns for the use of cisplatin and provide the impetus to explore other agents.

Detroit 562 is a pharyngeal squamous cell carcinoma with a gain-of-function mutant p53 that is due to a R175H amino acid substitution. The mutation resides on the L2 loop of the DNA-binding domain and is characterized by the overexpression of mutant p53 and the promotion of metastasis and mortality in a xenograft mouse model (14). In our previous effort to discover antiviral agents against poxvirus by disrupting the poxviral processivity factor, an indole-based small molecule (24a) was realized (15). The present study describes the discovery of 24a as a candidate anticancer agent for future studies. To accomplish this, the present study

Correspondence to: Professor Robert P. Ricciardi or Dr Manunya Nuth, Department of Basic and Translational Sciences, School of Dental Medicine, University of Pennsylvania, Levy Building, 4010 Locust Street, Philadelphia, PA 19104, USA
E-mail: ricciard@upenn.edu
E-mail: mnuth@upenn.edu

Key words: head and neck cancer, pharyngeal carcinoma, squamous cell carcinoma, small molecule, apoptosis, cell cycle

aimed to demonstrate the ability of 24a to promote antiproliferative and pro-apoptotic properties against an aggressive HNSCC-derived cell line. This was done using cell viability and cell cycle analysis studies and the probing of the expression profiles of various putative protein targets involved in cell proliferation and cell death. Of particular interest was the potential contribution of p53.

Materials and methods

Compounds. Cisplatin and nocodazole were purchased from Sigma-Aldrich; Merck KGaA. 24a was synthesized and confirmed by elemental analysis, liquid chromatography-mass spectrometry and nuclear magnetic resonance spectroscopy at >95% purity as previously described (15). Cisplatin was prepared in PBS. Nocodazole and 24a were prepared in DMSO.

Cells. The Detroit 562 cell line (cat. no. CCL-138) was obtained from the American Type Culture Collection (ATCC) and maintained in DMEM growth medium (Gibco; Thermo Fisher Scientific, Inc.), supplemented with 10% FBS (Corning, Inc.) and 25 μg/ml gentamicin (Gibco; Thermo Fisher Scientific, Inc.). Cells were confirmed negative for mycoplasma species by the MycoAlert detection kit (Cambrex Bio Science Rockland, Inc.) performed at the Department of Genetics Core at University of Pennsylvania. Genotyping was performed at the Core using standard methodology for short tandem repeat (STR) profiling in accordance with the American National Standards Institute's Authentication of Human Cell Lines: Standardization of STR Profiling (ANSI/ATCC ASN-0002-2011) at eight autosomal loci and amelogenin. Cells were authenticated by 93% match to the reference STR database of ATCC. Cells were cultured at 5% CO_2 in a humidified incubator at 37˚C. The normal fibroblast cell line, GM04390, was obtained from the Genetics Core and similarly maintained. B38 and BSC-1 cell lines (ATCC) were similarly maintained in 10% FBS/DMEM growth medium, HeLa cells (ATCC) were maintained in RPMI-1640 growth medium (Gibco; Thermo Fisher Scientific, Inc.) supplemented with 10% FBS and 25 μg/ml gentamicin, and MDA-MB-231 cells (ATCC) were maintained in Leibovitz's L-15 (Gibco; Thermo Fisher Scientific, Inc.) supplemented with 10% FBS and 25 μg/ml gentamicin. For all experiments, cells were not subjected to synchronization prior to compound treatments.

Cytotoxicity. Detroit 562 cells were seeded ~$8x10^3$ cells/well overnight in 96-well plates in 100 μl of growth medium to obtain 15-20% confluence at the time of treatment. For cisplatin treatment, PBS served as mock treatment. By comparison, nocodazole and 24a treatments were maintained at 1% DMSO throughout, with 1% DMSO serving as mock treatment. Compounds were serially diluted two-fold in growth media and prepared in triplicate. Fresh growth medium exchange occurred after 3 days. On the 6th day, cells typically reached 80-90% confluence, indicating at least two cell population doubling. Following treatment, 20 μl of 5 mg/ml 3-(4,5-dimethylthiazol-2-yl)-2,5-diphenyltetrazolium bromide (MTT, prepared in PBS) was added to each well, and the plate was incubated another 2 h in a humidified incubator at 37˚C. The growth media were then removed by aspiration, and the solid formazan in each well was dissolved in 150 μl of isopropanol containing 4 mM HCl and 0.1% P-20 by remaining for 1 h at room temperature. Absorbance was measured at 590 nm by a microplate reader. Cell viability was determined relative to the mock treatment and fitted by non-linear regression. Cell viability studies for GM04390A, B38, BSC-1, HeLa, and MDA-MB-231 were performed at the same plating density and processing (Fig. S1). Detection of cell viability was determined by staining with the nucleic acid-binding fluorescent dye, CyQUANT GR, according to the manufacture's recommendation (Invitrogen; Thermo Fisher Scientific, Inc.) and measured on a fluorescence microplate reader at 520 nm emission.

Cell cycle analysis. Cells were seeded at $1.3x10^6$ cells/dish overnight in six-cm dishes to yield ~40% confluence and then treated with 24a or 1% DMSO for 24 h. Following treatment, suspended cells were collected from growth media by centrifugation at 600 x g for 5 min at 25˚C. Adherent cells were washed with PBS, trypsinized and similarly collected by centrifugation as the suspended cells. Both cell collections were resuspended in PBS and pooled. Ice-cold ethanol was added to yield 70% final concentration and the cells were fixed by incubating at 4˚C for 2 h. The fixed cells were then collected by centrifugation at 600 x g for 5 min at 4˚C and rehydrated in PBS. The cells were next similarly collected by centrifugation, resuspended in 100 μl staining solution consisting of 15 μg/ml propidium iodide (PI), 10 μg/ml RNAse, 5 mM EDTA and 5 mg/ml BSA (Thermo Fisher Scientific, Inc.) in PBS and incubated overnight in the dark at 4˚C. The cells were then diluted with an addition of 300 μl PBS, filtered through a 100-μm mesh, and measured on a NovoCyte flow cytometer (ACEA Bioscience, Inc.) at 488-nm excitation and detection by the phycoerythrin channel, with no further compensation of the fluorescent signals. The cell cycle distribution was determined with the NovoExpress software version 1.3.0 (ACEA Bioscience, Inc.).

Construction of Detroit 562 cells expressing fluorescence ubiquitination-based cell cycle indicator (FUCCI). VSV-G pseudotyped lentiviral particles were generated from the transfection of 293T cells (ATCC) by the Lipofectamine® 3000 reagent (Invitrogen; Thermo Fisher Scientific, Inc.) according to the manufacturer's recommendation with the 3rd generation pBOB-EF1-FastFUCCI-Puro transfer vector (plasmid no. 86849), the 2nd generation packaging plasmid pCMV-dR8.2 dpr (plasmid no. 8455) and the 2nd generation envelope plasmid pCMV-VSV-G (plasmid no. 8454) obtained from Addgene, Inc. 293T cells (at ~95% confluence in a 10-cm dish) were transfected with 10 μg transfer vector, 5 μg packaging plasmid and 5 μg envelope plasmid and the media harvested 48 and 72 h post-transfection. For the generation of the FastFUCCI-expressing cells, Detroit 562 cells (~$2x10^5$ cells/well of a 24-well plate) were transduced with virus at 10 multiplicity of infection for 72 h and selected with 2 μg/ml puromycin over a 2-week period. Following puromycin selection, cells were diluted to allow the expansion of various clones and maintained at 1 μg/ml puromycin. Clonal expansion proceeded for another 2 weeks so as to generate cell stocks and enough cells for experimentation, totaling

31 days post-transduction. The expressed licensing factor Cdt1 was fused to the fluorescent protein, monomeric Kusabira Orange 2, to create the FUCCI reporter that allows visualization of cells in the G_1 phase. A fusion protein of geminin with fluorescent monomeric Azami Green allows for the monitoring of cells in the G_2 phase.

Microscopy. FastFUCCI-expressing Detroit 562 cells were seeded at $5x10^4$ cells and cultured in 35-mm glass dishes and the images were captured on a DMi8 fluorescence microscope (Leica Microsystems GmbH). For the assessment of membrane integrity, the cells were incubated at 37˚C with 10 μg/ml PI one hour prior to imaging.

Isothermal titration calorimetry (ITC). DNA-binding was measured by ITC on a MicroCal iTC200 instrument (Malvern Panalytical, Ltd.) as previously described (16). Briefly, fragmented salmon sperm DNA was dialyzed in 10 mM sodium phosphate, 0.15 M NaCl, pH 7.8 and prepared at 20 μg/ml concentration in the dialysate supplemented with 1% DMSO and 0.005% P-20 to serve as the ligand. The sample-representing buffer, 60 μM ethidium bromide (EtBr), or 100 μM 24a-was similarly prepared in the dialysate. Data are displayed as raw heat values without further deconvolution.

Protein extraction, protein array and western blot analysis. Detroit 562 cells were seeded at $5x10^6$ cells in a 15-cm dish and cultured to ~80% confluence. Cells were then trypsinized and seeded at ~$3x10^6$ cells/dish in nine 6-cm dishes, allowing for three dishes per treatment. After overnight growth and upon reaching ~80% confluence, the dishes were treated for 24 h with 0, 0.1 and 1 μM 24a at 37˚C. DMSO was maintained at 1% throughout. The suspended cells were then collected from growth media by centrifugation at 600 x g for 5 min at 25˚C. The adherent cells were washed twice with PBS and the cells from the washings were similarly collected. The non-ionic buffer supplied by the Proteome Profiler Human Apoptosis Array kit (cat. no. ARY009; lot no. 1487784; R&D Systems, Inc.) was supplemented with complete protease inhibitor cocktail and 1.5% phosphatase inhibitor cocktail 3 (both from Sigma-Aldrich; Merck KGaA); a total of 600 μl buffer was used to lyse the three plates representing each treatment. While keeping the cells on ice, cell lysis was aided by scraping with a cell scraper and subsequent sonication of the pooled fractions with six 5-sec pulses. After centrifugation for 10 min at 18,407 x g at 4˚C, the concentrations of the clarified lysates were determined by BCA method using BSA as standard. The lysates were aliquoted and stored at -80˚C until use. For protein profiling, the Apoptosis Array permitted the detection of 35 apoptosis-related proteins by antibodies spotted on nitrocellulose membranes. A total of 400 μg protein was used per membrane according to the manufacturer's protocol and visualized by chemiluminescent detection (using manufacturer's supplied reagents) on the Amersham Imager 680 instrument (Cytiva). Blot densitometry was analyzed using ImageJ software, version 1.53k (National Institutes of Health).

For western blot analysis, typically 10 or 20 μg total proteins were loaded into each well of a 4-12% Bis-Tris minigel and detected by standard western blot technique. Briefly, membranes were blocked for 1 h in 5% milk in TBS/0.1% Tween-20 at room temperature by rocking and incubated overnight with primary antibodies (prepared in blocking buffer) at 4˚C. The membranes were then washed three times with TBS/0.1% Tween-20 at room temperature and incubated with HRP-conjugated secondary antibody (prepared in blocking buffer) for 1 h and similarly washed. Antibodies against β-actin (cat. no. 4970), GAPDH (cat. no. 5174), death receptor (DR)4 (cat. no. 42533), DR5 (cat. no. 8074), DR6 (cat. no. 93026), Fas (cat. no. 4233), phosphorylated (p)-Atg1/ULK1 (cat. no. 6888), poly (ADP-ribose) polymerase 1 (PARP; cat. no. 9542) p53 (cat. no. 2527), p-p53 (cat. nos. 9288 for protein phosphorylation at Ser-9; 9284 at Ser-15; 2526 at Ser-33; and 9281 at Ser-392; cat. no. 2525 for protein acetylation at Lys-382), p63 (cat. no. 39692) p-p63 (cat. no. 4981, phosphorylation at Ser-160/162), p73 (cat. no. 14620) p-p73 (cat. no. 4665, phosphorylation at Tyr-99), Rip1 (cat. no. 3493), tumor necrosis factor receptors (TNFR)1 (cat. no. 3736) and TNFR2 (cat. no. 3727) were purchased from Cell Signaling Technology, Inc. Atg7 (cat. no. Ab133528) was purchased from Abcam and Beclin-1 (cat. no. NB500-249) was purchased from Novus Biologicals LLC. The primary antibodies were used at 1:1,000 dilution and the secondary antibody (anti-rabbit IgG, HRP-linked antibody; cat. no. 7074; Cell Signaling Technology, Inc.) at 1:4,000 dilution. Detection was performed by chemiluminescence using the SuperSignal West Pico PLUS reagent (Thermo Fisher Scientific, Inc.) and visualization on the Amersham Imager 680 instrument (Cytiva), followed by densitometry determination using ImageJ software.

Terminal deoxynucleotidyl transferase dUTP nick end labeling (TUNEL). Apoptotic cells were detected colorimetrically using the HT TiterTACS Apoptosis Detection kit (R&D Systems, Inc.). Detroit 562 cells were seeded overnight at ~$3x10^4$ cells per well in 96-well plates and treated at 37˚C the next day (~50% confluence at the time of treatment) with 2-fold serial dilutions of 24a, with 1% DMSO maintained throughout. After 24 h, the cells were processed and detected at 450 nm absorbance on a plate reader according to the manufacturer's instructions.

Caspase activity. Detroit 562 cells were seeded overnight in 6-cm dishes at ~$2x10^4$ cells per dish, resulting in ~40% cell confluence at the time of treatment. The growth media were removed and replaced with fresh growth media containing 0, 0.1 and 1.0 μM 24a, with DMSO maintained at 1% throughout. After 24 h, suspended cells were collected from the corresponding growth media by centrifugation at 25˚C at 600 x g for 5 min. The adherent cells were washed once with PBS, similarly collected and pooled with the cells collected from suspension. Cells from each treatment (pooled adherent and suspension fractions) were added with 500 μl of the supplied lysis buffer and lysed by two freeze-thaw cycles. Cell lysates were then clarified by centrifugation at 18,407 x g at 4˚C for 10 min and the protein concentrations were determined by BCA method. A total of 20 μg protein was used for each reaction according to the manufacturer's protocol. Caspase-3/7 activity was assessed by measuring the ability of the cell lysates to cleave the substrate DEDVpNA and produce the colorimetric pNA whose absorbance is measured at 405 nm (CaspACE Assay; Promega Corporation). Similarly,

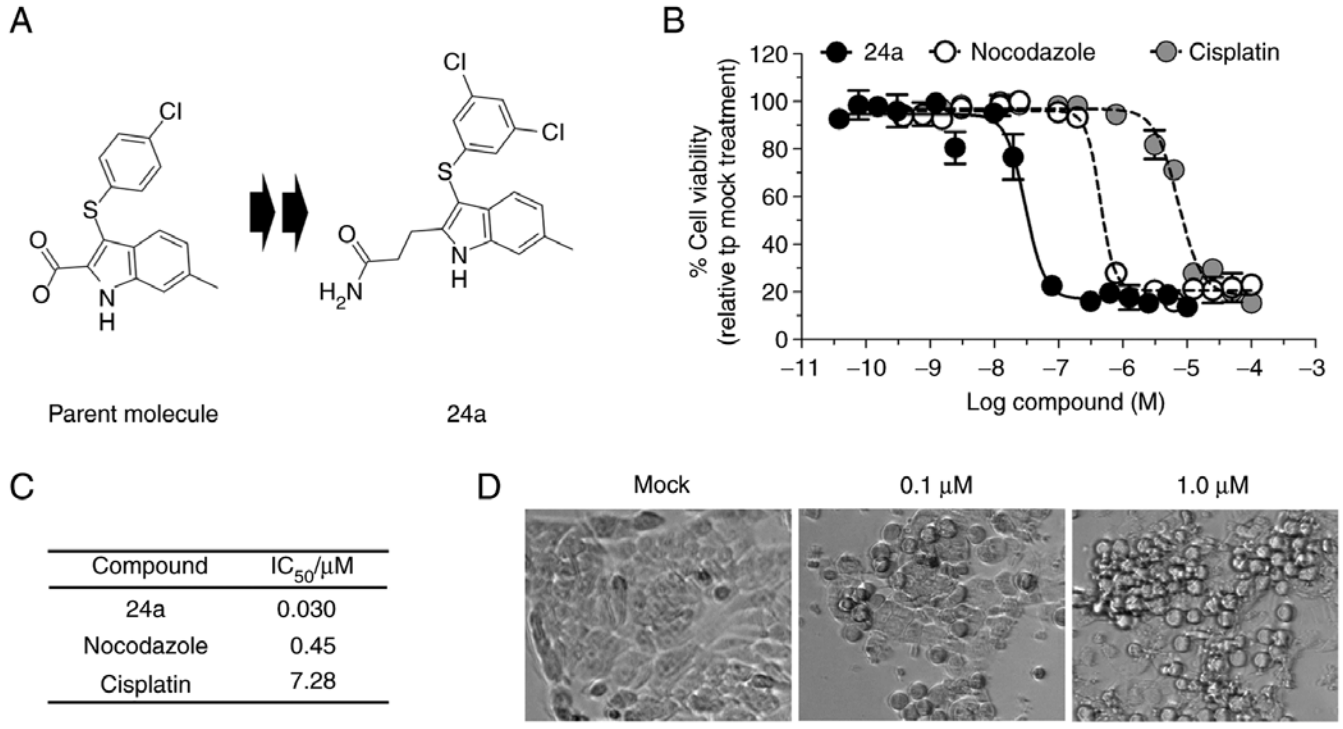

Compound	IC_{50}/μM
24a	0.030
Nocodazole	0.45
Cisplatin	7.28

Figure 1. 24a promotes potent cell death in Detroit 562 cells. (A) 24a was realized from compound optimization. (B and C) Growth inhibition by 24a. Cytotoxicity was measured following 6-day treatment. Values represent the mean ± SD of n=3. (D) Dose-dependent change in cell morphology following 24a treatment. Phase-contrast images were captured following 24-h treatment. As shown and referenced in the text, 0.1 and 1.0 μM 24a represent low and excess treatment doses, respectively. Magnification, x10.

the substrate AcVEIDpNA (Cayman Chemical Company) was used to measure caspase-6 activity.

Statistical analysis. Unless indicated, mean ± standard deviation values were obtained from triplicate experiments. The comparison of 24a treatments with corresponding mock treatments were analyzed using Prism software (version 5; GraphPad Software, Inc.), using one-way analysis of variance with post hoc Tukey's test. $P<0.05$ was considered to indicate a statistically significant difference.

Results

Identification of 24a as a potent cytotoxic agent. A previous screen of small molecules against vaccinia virus (VACV) has identified an indole-based scaffold from which optimization steps are performed to produce antiviral pox therapeutics (15). While the optimized propanamide 24a (Fig. 1A) proves to have a potent antiviral activity against VACV infection, it also exhibits appreciable cytotoxicity, effectively eliminating the African green monkey kidney epithelial cells (BSC-1) at a half-maximal inhibitory concentration (IC_{50}) of 16 μM following 24-h exposure (15). Investigation into longer exposure (72 h) of 24a with various tumor cell lines unexpectedly revealed the promotion of growth inhibition well into the nanomolar concentrations (Fig. S1). Therefore, it was sought to explore whether 24a was equally effective at inhibiting cell growth of an HNSCC cell line.

The viability of Detroit 562 cells was measured following 6 days of treatment, which equated to at least 2 doubling of cell populations observed in the mock treatment. Indeed, 24a showed potent growth inhibition, with an extracted IC_{50}=0.03 μM (Fig. 1B and C). By comparison, the antimitotic agent nocodazole and the chemotherapeutic agent cisplatin inhibited the proliferation of Detroit 562 cells at IC_{50} values of 0.45 and 7.28 μM, respectively (Fig. 1B and C). When the cells were visualized following a shorter treatment time (24 h), morphological changes were evident in a dose-dependent manner (Fig. 1D), with the round and shrunken cells suggestive of apoptotic events (17).

24a promotes G_2/M blockade. Since the potent growth inhibitory effect of 24a was only observed after an extended treatment time, the effect on the cell cycle was suspected and therefore examined. To accomplish this, Detroit 562 cells were treated with 1 and 5 μM 24a for 24 h and characterized by flow cytometry after nuclear staining with propidium iodide (PI). In comparison with the mock treatment, the observed accumulation of cell populations in the G_2 phase was 1.8- and 1.9-fold for 1 and 5 μM 24a treatments, respectively (Figs. 2A and S2). In addition, the accumulation of subG_1 cell populations further hinted at the promotion of apoptosis. By comparison, 5 μM 24a failed to accumulate normal fibroblasts (GM04390) in either the G_1 or G_2 phase (Figs. 2A and S2), suggesting the sparing of cells that were not as proliferative.

Next, it was sought to examine whether the G_2/M blockade could play a role in cell death. To investigate real-time cell cycle progression, Detroit 562 cells expressing the FUCCI were prepared from VSV-G pseudotyped lentiviral particles produced by the all-in-one expression cassette, FastFUCCI (18). By monitoring the protein levels of the licensing factor Cdt1 (which peaks during G_1 and decreases

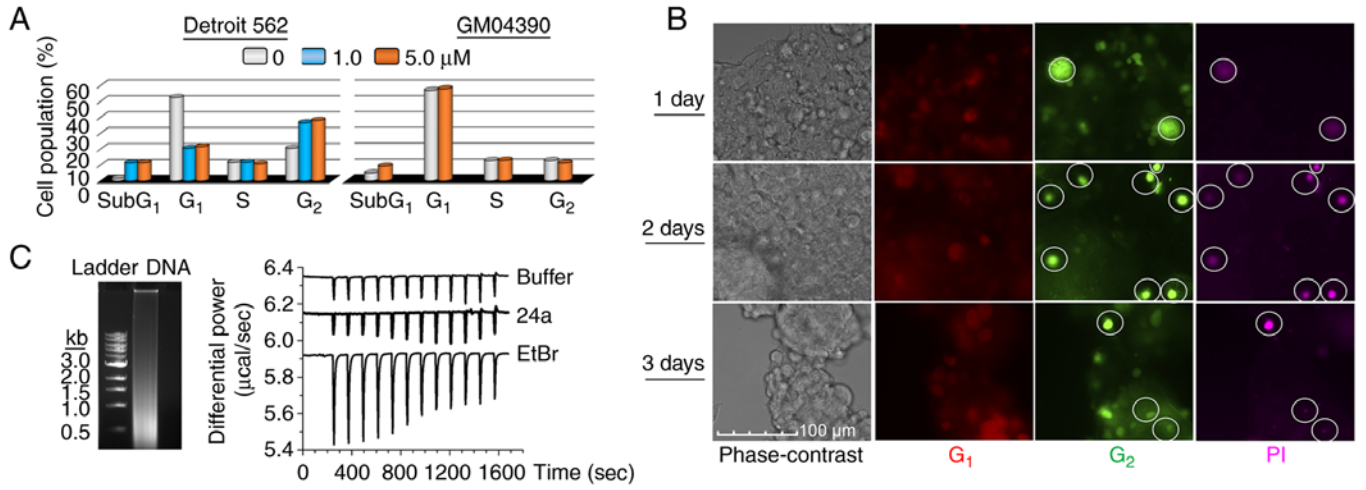

Figure 2. Detroit 562 cells arrested in the G_2 phase are susceptible to cell death. (A) Examination of the cell cycle in response to 24a treatment. Cell cycle distribution was determined by flow cytometric analysis of PI-stained cells following 24-h treatment at the indicated doses. GM04390 is normal human fibroblasts. Values represent the mean of n=2. (B) Examination of real-time cell cycle progression using FastFUCCI-expressing Detroit 562 cells. A fusion protein of Cdt1 and monomeric Kusabira Orange 2 creates the FUCCI reporter that allows visualization of cells in the G_1 phase. A fusion of geminin with monomeric Azami Green allows for the monitoring of cells in the G_2 phase. Cells were treated with 0.03 μM 24a for the indicated duration and PI was added 1 h prior to imaging. As shown circled, only cells arrested in the G_2 phase also stained for PI. Magnification, x20. (C) Assessment of compound binding by isothermal titration calorimetry. Random, fragmented DNA was titrated into a sample of buffer, 60 μM EtBr or 100 μM 24a. Raw heat values without further deconvolution are demonstrated. PI, propidium iodide; EtBr, ethidium bromide; FUCCI, fluorescence ubiquitination-based cell cycle indicator.

entering S phase) and its inhibitor geminin (which peaks during S, G_2, and M phases, but decreases during late mitosis and G_1), DNA replication could be monitored in live cells (19). The FastFUCCI-expressing Detroit 562 cells were treated with 0.03 μM 24a (at a low concentration value that permitted the following of cell progression without markedly causing cell death) and monitored 1-, 2- and 3-days post-treatments. At 1 h prior to microscopy, PI was directly added to the growth medium to assess membrane integrity. Compared with the undetectable PI-staining of the mock-treated cells (Fig. S3), the cell-impermeant PI specifically stained 24a-treated cells in the G_2 phase (Fig. 2B). The absence of PI-staining of cells in the G_1 phase provided support that only cells that progressed to the G_2 phase lost membrane integrity and were susceptible to cell death.

Finally, the lack of G_1/S blockade by 24a treatment would presumably argue against promiscuous DNA-binding as a possible mode-of-action. To ensure that this was indeed the case, direct DNA-binding was investigated by ITC. As expected, the DNA-intercalating EtBr was able to generate a binding thermogram when titrated with random, fragmented DNA, while 24a only generated a thermogram similar to that of buffer alone, thus indicating the lack of associated binding events (Fig. 2C). Taken together, 24a effectively promoted growth arrest by G_2/M blockade and cells experiencing this blockade were susceptible to cell death.

The promotion of apoptosis as the key underlying mode of cell death. To gain insight into the mode of cell death, protein markers of necrosis (Rip1) and autophagy (p-Atg1, Atg7 and Beclin-1) were initially examined by western blot analysis. As revealed in Fig. 3A, the levels of all investigated proteins either remained unchanged or decreased when treated with 0.1 (low) and 1.0 μM (excess) 24a. Next, TUNEL assay was performed following 24 h treatment to assess the endpoint of apoptosis. Overall, the promotion of apoptosis was observed over the mock treatment in all test concentrations; a non-monotonic trend was exhibited by the increase of TUNEL response for up to 0.25 μM 24a followed by decreasing response from 0.5-2 μM 24a (Fig. 3D). In accordance with the TUNEL results, both caspase-3/7 and caspase-6 activities were significantly increased with increasing 24a concentrations compared with mock treatments (Fig. 3B and C), demonstrating these effector caspases as important contributors of apoptosis. Notably, excess 24a consistently produced decreasing caspase activities compared with the low dose, an observation consistent with the decreasing TUNEL response at the same treatment concentration, together implicating apoptosis as an important event at the low dose. Given that poly (ADP-ribose) polymerase 1 (PARP) is a target of caspases-3, -6 and -7 (20,21), PARP protein levels were further assessed. Indeed, dose-dependent cleavage of PARP was observed following 24a treatment (Figs. 3E and 4C).

24a promotes the increase in expression of DRs. Given that apoptosis plays an important role in the observed cytotoxicity, it was next sought to gain insight into the involvement of possible signaling proteins. To accomplish this, Detroit 562 cells were treated with low and excess doses of 24a for 24 h and the lysates were specifically probed for apoptosis-related proteins using the Human Apoptosis Array (Fig. S4). It is worth noting that a longer incubation time was not investigated due to the depletion of cell populations and the likely introduction of confounding cell death events (data not shown). Out of the 35 apoptosis-related proteins simultaneously probed in the array, only the response from the DRs was appreciable, with quantifiable increase in the expression levels of DR4 and DR5 compared with the mock treatment (Fig. 4A and D). Western blot analysis was further used to confirm the DR4 and DR5 results and to sample other possible DRs that either

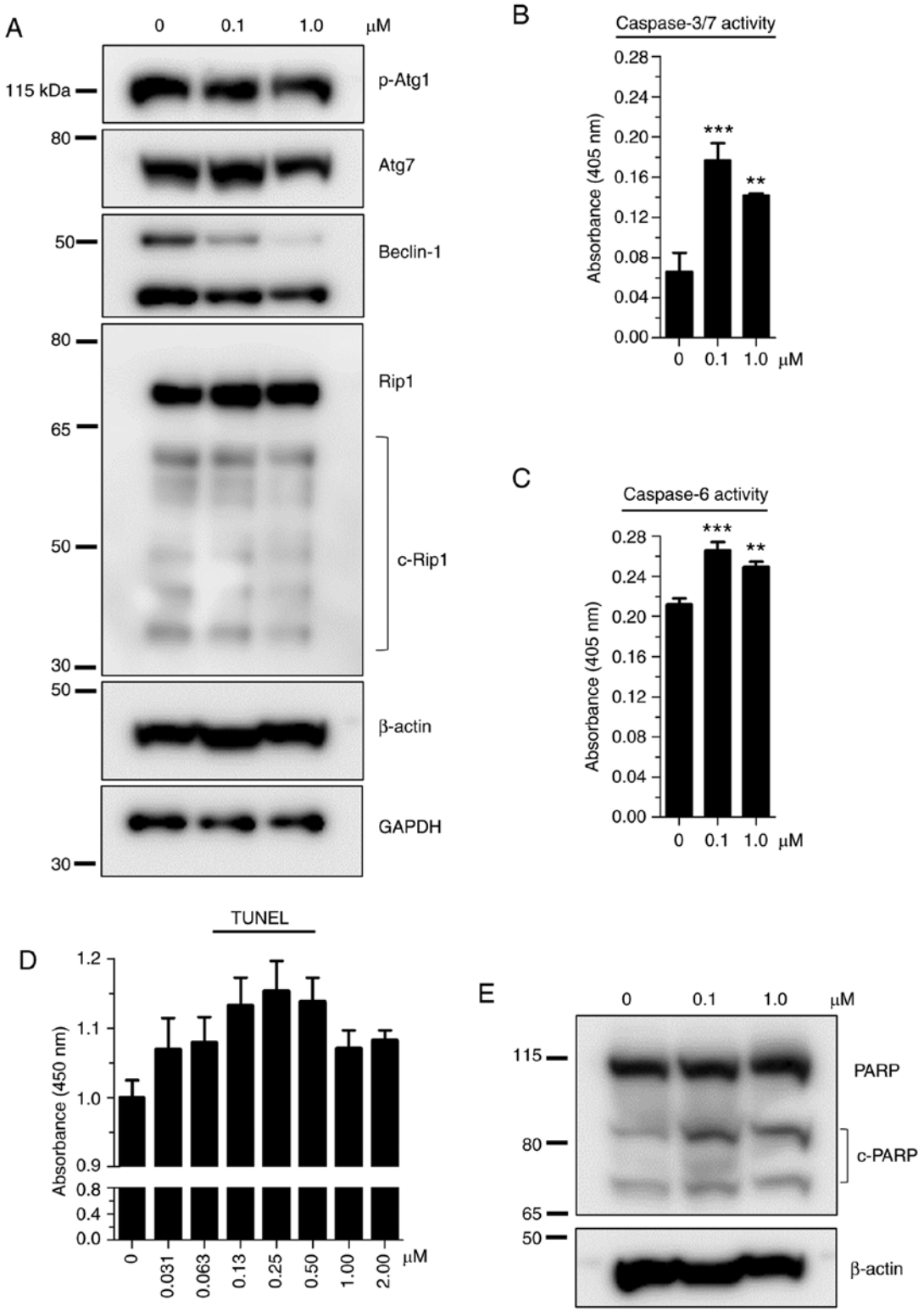

Figure 3. Examination of the effect of 24a on the markers of autophagy, necrosis and apoptosis following 24 h treatment. (A) Demonstration of the lack of (or negligible) response from markers of necrosis and autophagy. Cell lysates were prepared from Detroit 562 cells treated with 24a at the indicated doses. As determined by western blot analysis, p-Atg1, Atg7 and Beclin-1 represent protein markers of autophagy and Rip1 is a marker of necrosis. Representative blots of duplicate experiments are shown, with the typical β-actin as loading control for p-Atg1 and Atg7 and GAPDH as loading control for Beclin-1 and Rip1. Supporting evidence for apoptosis following 24a treatment by (B) caspase-3/7 and (C) caspase-6 activities, (D) TUNEL assay, and (E) the cleavage of PARP protein. Values represent the mean ± SD of n=3, with the treatment values compared with that of the corresponding mock values. **P<0.01 and ***P<0.001 vs. 0 μM control. p-, phosphorylated; c-, cleaved; PARP, poly (ADP-ribose) polymerase 1.

gave weak responses between the mock and treatments or were not included in the array. Accordingly, both DR4 and DR5 showed a dose-dependent increase in protein levels following 24a treatment (Fig. 4B and C). Another DR that was not included among the array probes, DR6, also showed dose-dependent increase in expression when exposed to 24a

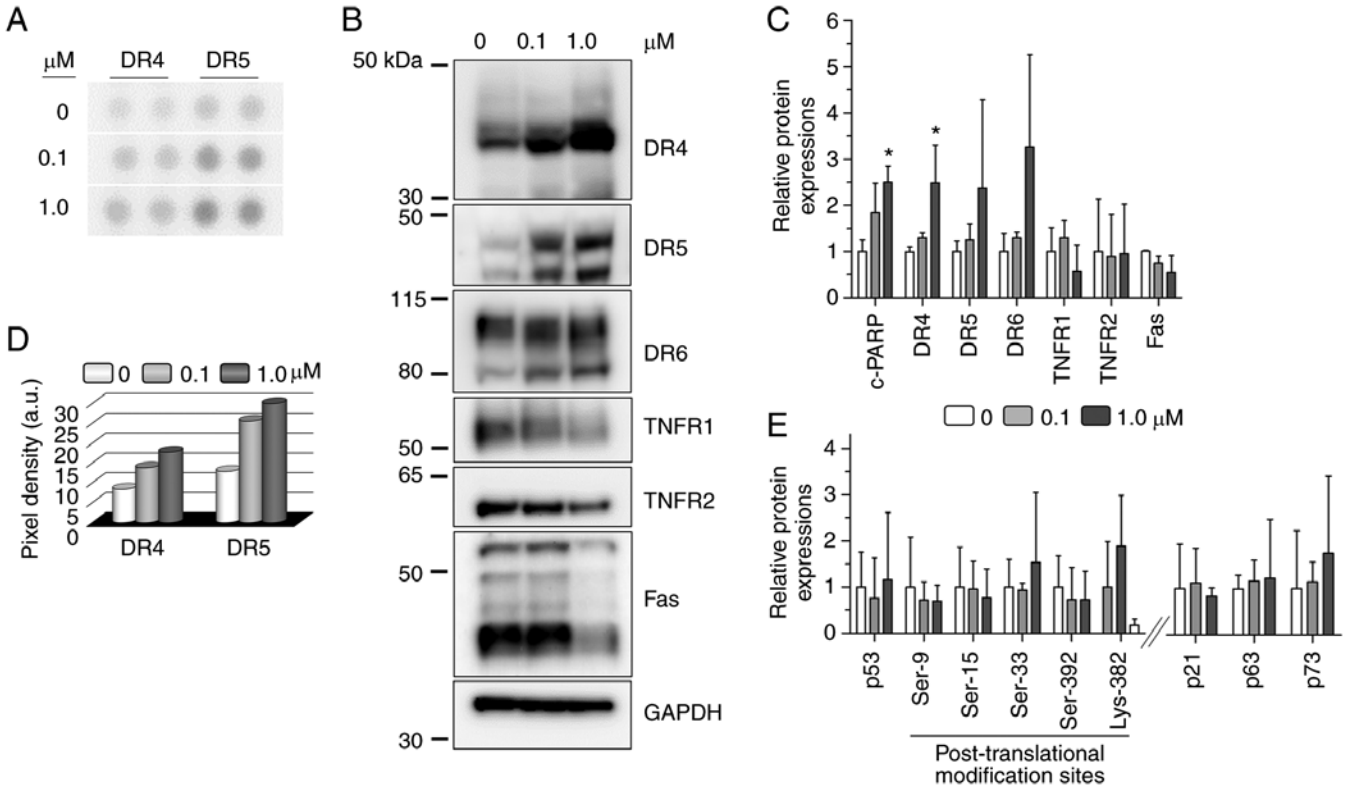

Figure 4. 24a promotes the expression of DRs. Cell lysates were prepared from Detroit 562 cells treated with 24a for 24 h at the indicated doses. (A) Human Apoptosis Array permitted the probing of 35 apoptosis-related proteins by antibodies spotted in duplicates on nitrocellulose membranes. Representative images of chemiluminescence spots corresponding to DR4 and DR5 are demonstrated. (B) Western blot results depicting DR expression levels. Representative blots are shown, with GAPDH depicting the typical loading control. (C) Relative protein expressions are quantified from blots determined in B and Fig. 3E for c-PARP. (D and E) Summary of the relative protein expressions of total p53, p53 proteins at various post-translational modification sites, p21, p63 and p73 determined from representative blots shown in Fig. S5. Values represent the mean ± SD of n=3, with the treatment values compared with that of the corresponding mock values. *P<0.05 vs. 0 μM control. DR, death receptor; c-, cleaved; PARP, poly (ADP-ribose) polymerase 1; TNFR, tumor necrosis factor receptor.

(Fig. 4B and C). In agreement with the array, TNFR1 and Fas showed negligible to decreasing change in protein levels following treatments (Fig. 4B and C). Similarly, a random examination of TNFR2 (which is not included among the array probes) showed negligible change in protein levels in response to 24a (Fig. 4B and C). Taken together, the results from the Apoptosis Array and independent probing by western blot consistently showed 24a to specifically promote the expression of DR4, DR5 and (to an extent) DR6 in response to 24a treatment for both low and excess doses, while the other tumor necrosis factor (TNF) superfamily members examined (TNFR1, TNFR2 and Fas) were not responsive.

24a does not promote p53, p63 and p73 activities. When cells are stressed or damaged, the tumor suppressor p53 is an important transcriptional activator of target genes that invoke apoptosis, senescence and cell cycle arrest. However, the majority of human cancers contain incorrectly functioning p53, with ~1/2 of these cancers owing to the inactivation of the p53 protein as the result of mutations to the TP53 gene (22). In particular, 68.2% of cell lines derived from an oral and pharyngeal cancer panel have been demonstrated to exhibit TP53 mutations (8). Among the squamous cell carcinoma cell lines, G>T (or an alternate G>A) transversion is commonly observed concomitantly with the overexpression of p53 (23). Indeed, a c.524G>A transversion results in the amino acid R175H substitution that endows Detroit 562 with a gain-of-function p53 that promotes tumor growth and metastasis (14). In the present study, it was sought to determine whether p53 was activated in response to 24a. Since the effect of p53 on cellular functions largely requires post-translational modifications at more than a single site (24,25), the status of various putative phosphorylation and acetylation sites was investigated. As summarized in Fig. 4E and shown in Fig. S5, western blot results showed the total protein levels of p53 and its post-translationally modified forms remained constant following 24a treatment.

Next, the protein levels of the p53 paralogs (p63 and p73) were examined to assess their potential contributions. While the wild-type proteins can serve redundant functions to p53, differential promoter activation and splicing can generate dominant negative (ΔN) isoforms that lack the transactivation function, thereby counteracting the tumor suppressive function of p53. Given that p63 and p73 are rarely mutated, tumorigenesis is then reflected by the expression levels of these ΔN isoforms relative to the wild-type proteins (26). For example, the alpha isoform of ΔNp63 is observed predominantly overexpressed in HNSCC (27) and likely contributes to oncogenesis (28). Similarly, the expression of the ΔNp73 isoforms also endows antiapoptotic and proliferative properties (29). As summarized in Fig. 4E and shown in Figs. S5 and S6 for Detroit 562 cell lysates, the observed faster-migrating bands

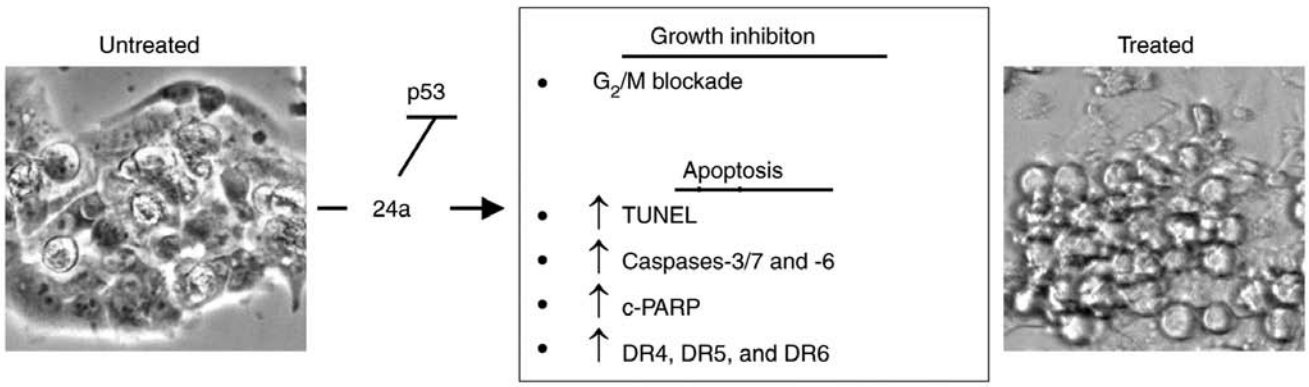

Figure 5. Summary of the proposed action of 24a on Detroit 562 cells: Cytotoxic effect is promoted independent of p53. Following 24-h treatment, 24a shows the ability to promote cell cycle arrest at the G_2/M phase as demonstrated by flow cytometric analysis. Change in cell morphology and the observed increase of subG1 cell populations shown in Fig. 2A hint at the promotion of apoptosis. Accordingly, the promotion of TUNEL-staining with the concomitant increase of caspase activities and the relative increase in the protein levels of cleaved PARP and DRs provide support of apoptosis. PARP, poly (ADP-ribose) polymerase 1; TUNEL, terminal deoxynucleotidyl transferase dUTP nick end labeling; DR, death receptor; c-, cleaved-.

on the gels are more in line with the expression of the ΔN isoforms of both p63 and p73. As such, the negligible change in the expression levels following 24a treatment indicated the lack of contribution by both proteins. In addition, 24a treatment produced no detectable protein phosphorylation for either p63 at Ser-160/162 or p73 at Tyr-99 (Fig. S6), further indicating the lack of contribution from either p63 or p73 on the basis of phosphorylation status.

As a target of p53, $p21^{WAF1/CIP1}$ can suppress the growth of various tumor cell lines (30). Therefore, its presence is considered indicative of wild-type p53 function (31). Accordingly, it was sought to examine corresponding p21 protein levels in response to 24a treatment. As summarized in Fig. 4E and shown in Fig. S5, p21 protein levels did not increase in a dose-dependent manner following 24a treatment, further ruling out the involvement of p53.

Discussion

Squamous cell carcinoma is the major form of malignancy that arises in head and neck cancer and is challenging to treat largely due to the detection of locally advanced diseases (32). While surgery is recommended for early-stage diseases, there is the need to avoid or minimize undue morbidity and promote organ preservation (13). Such that unresectable tumors are largely accessible by radiotherapy and chemotherapy, it follows that the curative effort therefore must adopt multipronged strategies whereby various drugs, in combination, attempt to disrupt the various signaling events required by the cancer. Indeed, cytotoxic agents remain the inevitable treatment options for advanced cancers and metastases (33).

Cisplatin is a commonly used and important cytotoxic agent that, through the aquation reaction (34), produces a highly potent electrophile that can react to nucleophiles such as protein thiols and nitrogen donor ligands of nucleic acid. Specifically, the crosslinking of cisplatin to purines blocks cell division, interferes with DNA repair and results in apoptosis, making it effective against various cancers, including bladder, head and neck, lung, ovarian and testicular cancers (12). Given the ability of cisplatin to block non-homologous end joining in DNA repair (35), the concurrent treatment with DNA-damaging radiation demonstrates cisplatin to be an effective radiosensitizer for improving survival and reducing recurrence in the management of unresectable HNSCC tumors (13). In another example, the combination of cisplatin with 5-fluoruracil (another cytotoxic agent that disrupts DNA synthesis) (36) and cetuximab (a monoclonal antibody against epidermal growth factor receptor, which is a marker of HNSCC) (37) represents an important first-line treatment of recurrent and metastatic HNSCC tumors (38). However, with the improvement of overall survival at only 10.1 months after this advanced treatment strategy, it argues for the need to explore other options (39).

In the present study, 24a was identified as a potent growth inhibitor against various tumor cell lines and specifically described its cytotoxic action against a human pharyngeal carcinoma cell line as owing to its antiproliferative and pro-apoptotic properties (Fig. 5). Its effectiveness appears to be largely due to the promotion of apoptosis in cell populations arrested in the G_2 phase. Furthermore, the promotion of the expression of DR4 and DR5 could prove interesting. Given that TRAIL promotes apoptosis in various tumor cell lines and is viewed as a promising anticancer avenue (40), the potential utility of 24a to promote synergy with TRAIL in a combination treatment could represent one intriguing aspect for future studies.

To shed light on the underlying mechanism-of-action of 24a, the tumor suppressor p53 was investigated due to its contribution to the control of both the cell cycle and apoptosis, as well as its role in the upregulation of DRs (41,42). Its importance is exemplified by the fact that TP53 mutations are associated with poor prognosis for patients with HNSCC (7). Therefore, it was sought to explore whether 24a could prove effective against an HNSCC cell model with a known TP53 mutation. To this end, Detroit 562 serves such a purpose, as the R175H mutation endows the cell line with a gain-of-function p53 that is responsible for aggressive tumor growth and metastasis (14). Accordingly, the R175H mutation represents a key hot spot found in numerous human cancers (43) and has been revealed to promote genomic instability in a mouse model (44). As such, it was asked whether the effectiveness

of 24a could be due to the promotion of p53 activity. This could be possible either by the restoration of wild-type function through the reactivation of the R175H mutant or the favoring of the residual wild-type p53 over the mutant protein. Indeed, the suppression of tumorigenesis by wild-type activities was observed for a heterozygous R175H mutant (44), and Detroit 562 is of unknown zygosity according to the Catalogue of Somatic Mutations (https://cancer.sanger.ac.uk/cosmic). However, the present findings do not support the involvement of p53, as evidenced by the lack of increase in the levels of post-translationally modified p53 proteins or its downstream effector p21. Additionally, no contribution was observed from its paralogs p63 and p73.

In summary, the present study revealed that 24a is a potent cytotoxic agent against malignant human pharyngeal squamous carcinoma cells *in vitro*. Accordingly, the exhibited growth inhibitory and pro-apoptotic properties appear to be due to signaling pathway(s) independent of p53. As such, future studies will be required to precisely identify the primary cellular target of 24a. Additionally, eventual testing in an animal tumor model will be required to demonstrate efficacy. In conclusion, 24a was identified as a promising anticancer candidate that warrants future studies.

Acknowledgements

Not applicable.

Funding

The present study was supported by The National Institute of Allergy and Infectious Diseases (grant no. U01AI082211) and The Joseph and Josephine Rabinowitz Award (School of Dental Medicine Institutional Grant).

Availability of data and materials

The datasets used and/or analyzed during the current study are available from the corresponding authors on reasonable request.

Authors' contributions

MN conceived and designed the study. MN, MRB and RPR analyzed and interpreted the data. MN and MRB performed all the experiments. MN, MRB and RPR confirm the authenticity of all the raw data. MN wrote the manuscript. All authors have read and approved the final manuscript.

Ethics approval and consent to participate

Not applicable.

Patient consent for publication

Not applicable.

Competing interests

The authors declare that they have no competing interests.

References

1. Vigneswaran N and Williams MD: Epidemiologic trends in head and neck cancer and aids in diagnosis. Oral Maxillofac Surg Clin North Am 26: 123-141, 2014.
2. Brennan JA, Boyle JO, Koch WM, Goodman SN, Hruban RH, Eby YJ, Couch MJ, Forastiere AA and Sidransky D: Association between cigarette smoking and mutation of the p53 gene in squamous-cell carcinoma of the head and neck. N Engl J Med 332: 712-717, 1995.
3. D'Souza G, Kreimer AR, Viscidi R, Pawlita M, Fakhry C, Koch WM, Westra WH and Gillison ML: Case-control study of human papillomavirus and oropharyngeal cancer. N Engl J Med 356: 1944-1956, 2007.
4. Bray F, Ferlay J, Soerjomataram I, Siegel RL, Torre LA and Jemal A: Global cancer statistics 2018: GLOBOCAN estimates of incidence and mortality worldwide for 36 cancers in 185 countries. CA Cancer J Clin 68: 394-424, 2018.
5. Hanahan D and Weinberg RA: Hallmarks of cancer: The next generation. Cell 144: 646-674, 2011.
6. Haddad RI and Shin DM: Recent advances in head and neck cancer. N Engl J Med 359: 1143-1154, 2008.
7. Poeta ML, Manola J, Goldwasser MA, Forastiere A, Benoit N, Califano JA, Ridge JA, Goodwin J, Kenady D, Saunders J, *et al*: TP53 mutations and survival in squamous-cell carcinoma of the head and neck. N Engl J Med 357: 2552-2561, 2007.
8. Martin D, Abba MC, Molinolo AA, Vitale-Cross L, Wang Z, Zaida M, Delic NC, Samuels Y, Lyons JG and Gutkind JS: The head and neck cancer cell oncogenome: A platform for the development of precision molecular therapies. Oncotarget 5: 8906-8923, 2014.
9. Algazi AP and Grandis JR: Head and neck cancer in 2016: A watershed year for improvements in treatment? Nat Rev Clin Oncol 14: 76-78, 2017.
10. Siegel RL, Miller KD, Fuchs HE and Jemal A: Cancer statistics, 2021. CA Cancer J Clin 71: 7-33, 2021.
11. Bar-Ad V, Palmer J, Yang H, Cognetti D, Curry J, Luginbuhl A, Tuluc M, Campling B and Axelrod R: Current management of locally advanced head and neck cancer: The combination of chemotherapy with locoregional treatments. Semin Oncol 41: 798-806, 2014.
12. Dasari S and Tchounwou PB: Cisplatin in cancer therapy: Molecular mechanisms of action. Eur J Pharmacol 740: 364-378, 2014.
13. Hartner L: Chemotherapy for oral cancer. Dent Clin North Am 62: 87-97, 2018.
14. Sano D, Xie TX, Ow TJ, Zhao M, Pickering CR, Zhou G, Sandulache VC, Wheeler DA, Gibbs RA, Caulin C and Myers JN: Disruptive TP53 mutation is associated with aggressive disease characteristics in an orthotopic murine model of oral tongue cancer. Clin Cancer Res 17: 6658-6670, 2011.
15. Nuth M, Guan H, Zhukovskaya N, Saw YL and Ricciardi RP: Design of potent poxvirus inhibitors of the heterodimeric processivity factor required for viral replication. J Med Chem 56: 3235-3246, 2013.
16. Nuth M, Guan H, Xiao Y, Kulp JL III, Parker MH, Strobel ED, Isaacs SN, Scott RW, Reitz AB and Ricciardi RP: Mutation and structure guided discovery of an antiviral small molecule that mimics an essential C-Terminal tripeptide of the vaccinia D4 processivity factor. Antiviral Res 162: 178-185, 2019.
17. Elmore S: Apoptosis: A review of programmed cell death. Toxicol Pathol 35: 495-516, 2007.
18. Koh SB, Mascalchi P, Rodriguez E, Lin Y, Jodrell DI, Richards FM and Lyons SK: A quantitative FastFUCCI assay defines cell cycle dynamics at a single-cell level. J Cell Sci 130: 512-520, 2017.
19. Sakaue-Sawano A, Kurokawa H, Morimura T, Hanyu A, Hama H, Osawa H, Kashiwagi S, Fukami K, Miyata T, Miyoshi H, *et al*: Visualizing spatiotemporal dynamics of multicellular cell-cycle progression. Cell 132: 487-498, 2008.
20. Kaufmann SH, Desnoyers S, Ottaviano Y, Davidson NE and Poirier GG: Specific proteolytic cleavage of poly(ADP-ribose) polymerase: An early marker of chemotherapy-induced apoptosis. Cancer Res 53: 3976-3985, 1993.
21. Chaitanya GV, Alexander JS and Babu PP: PARP-1 cleavage fragments: Signatures of cell-death proteases in neurodegeneration. Cell Commun Signal 8: 31, 2010.
22. Vogelstein B, Lane D and Levine AJ: Surfing the p53 network. Nature 408: 307-310, 2000.

23. Somers KD, Merrick MA, Lopez ME, Incognito LS, Schechter GL and Casey G: Frequent p53 mutations in head and neck cancer. Cancer Res 52: 5997-6000, 1992.
24. Giaccia AJ and Kastan MB: The complexity of p53 modulation: Emerging patterns from divergent signals. Genes Dev 12: 2973-2983, 1998.
25. Bode AM and Dong Z: Post-translational modification of p53 in tumorigenesis. Nat Rev Cancer 4: 793-805, 2004.
26. Deyoung MP and Ellisen LW: p63 and p73 in human cancer: Defining the network. Oncogene 26: 5169-5183, 2007.
27. Sniezek JC, Matheny KE, Westfall MD and Pietenpol JA: Dominant negative p63 isoform expression in head and neck squamous cell carcinoma. Laryngoscope 114: 2063-2072, 2004.
28. Nylander K, Coates PJ and Hall PA: Characterization of the expression pattern of p63α and δnp63α in benign and malignant oral epithelial lesions. Int J Cancer 87: 368-372, 2000.
29. Bisso A, Collavin L and Del Sal G: p73 as a pharmaceutical target for cancer therapy. Curr Pharm Des 17: 578-590, 2011.
30. el-Deiry WS, Tokino T, Velculescu VE, Levy DB, Parsons R, Trent JM, Lin D, Mercer WE, Kinzler KW and Vogelstein B: WAF1, a potential mediator of p53 tumor suppression. Cell 75: 817-825, 1993.
31. Georgakilas AG, Martin OA and Bonner WM: p21: A two-faced genome guardian. Trends Mol Med 23: 310-319, 2017.
32. Leemans CR, Braakhuis BJM and Brakenhoff RH: The molecular biology of head and neck cancer. Nat Rev Cancer 11: 9-22, 2011.
33. Bailly C, Thuru X and Quesnel B: Combined cytotoxic chemotherapy and immunotherapy of cancer: Modern times. NAR Cancer 2: zcaa002, 2020.
34. Knox RJ, Friedlos F, Lydall DA and Roberts JJ: Mechanism of cytotoxicity of anticancer platinum drugs: Evidence that cis-di amminedichloroplatinum(II) and cis-diammine-(1,1-cyclobutanedicarboxylato)platinum(ii) differ only in the kinetics of their interaction with dna. Cancer Res 46: 1972-1979, 1986.
35. Boeckman HJ, Trego KS and Turchi JJ: Cisplatin sensitizes cancer cells to ionizing radiation via inhibition of nonhomologous end joining. Mol Cancer Res 3: 277-285, 2005.
36. Grem JL: 5-Fluorouracil: Forty-plus and still ticking. A review of its preclinical and clinical development. Invest New Drugs 18: 299-313, 2000.
37. Bossi P, Resteghini C, Paielli N, Licitra L, Pilotti S and Perrone F: Prognostic and predictive value of EGFR in head and neck squamous cell carcinoma. Oncotarget 7: 74362-74379, 2016.
38. Vermorken JB, Mesia R, Rivera F, Remenar E, Kawecki A, Rottey S, Erfan J, Zabolotnyy D, Kienzer HR, Cupissol D, *et al*: Platinum-based chemotherapy plus cetuximab in head and neck cancer. N Engl J Med 359: 1116-1127, 2008.
39. Pendleton KP and Grandis JR: Cisplatin-based chemotherapy options for recurrent and/or metastatic squamous cell cancer of the head and neck. Clin Med Insights Ther 2013: 10.4137/CMT.S10409, 2013.
40. Johnstone RW, Frew AJ and Smyth MJ: The TRAIL apoptotic pathway in cancer onset, progression and therapy. Nat Rev Cancer 8: 782-798, 2008.
41. Wu GS, Burns TF, McDonald ER III, Jiang W, Meng R, Krantz ID, Kao G, Gan DD, Zhou JY, Muschel R, *et al*: KILLER/DR5 is a DNA damage-inducible p53-regulated death receptor gene. Nat Genet 17: 141-143, 1997.
42. Sheikh MS and Fornace AJ Jr: Death and decoy receptors and p53-mediated apoptosis. Leukemia 14: 1509-1513, 2000.
43. Hainaut P and Hollstein M: p53 and human cancer: The first ten thousand mutations. Adv Cancer Res 77: 81-137, 2000.
44. Liu DP, Song H and Xu Y: A common gain of function of p53 cancer mutants in inducing genetic instability. Oncogene 29: 949-956, 2010.